Topology in Nonlinear Mechanical Systems

Po-Wei Lo[®], ¹ Christian D. Santangelo, ² Bryan Gin-ge Chen, ³ Chao-Ming Jian, ¹

Krishanu Roychowdhury, ⁴ and Michael J. Lawler[®], ¹.

Laboratory of Atomic and Solid State Physics, Cornell University, Ithaca, New York 14853, USA

²Department of Physics, Syracuse University, Syracuse, New York 13244, USA

³Department of Physics and Astronomy, University of Pennsylvania, Philadelphia, Pennsylvania 19104, USA

⁴Department of Physics, Stockholm University, SE-106 91 Stockholm, Sweden

⁵Department of Physics, Applied Physics and Astronomy, Binghamton University, Binghamton, New York 13902, USA

(Received 26 April 2021; accepted 13 July 2021; published 13 August 2021)

Many advancements have been made in the field of topological mechanics. The majority of the work, however, concerns the topological invariant in a linear theory. In this Letter, we present a generic prescription to define topological indices that accommodates nonlinear effects in mechanical systems without taking any approximation. Invoking the tools of differential geometry, a ℤ-valued quantity in terms of a topological index in differential geometry known as the Poincaré-Hopf index, which features the topological invariant of nonlinear zero modes (ZMs), is predicted. We further identify one type of topologically protected solitons that are robust to disorders. Our prescription constitutes a new direction of searching for novel topologically protected nonlinear ZMs in the future.

DOI: 10.1103/PhysRevLett.127.076802

Mechanical systems offer a remarkable connection between physics and engineering. Through their simplicity, they have inspired both ideas at the foundation of theoretical physics and a sense of control over our physical world. In the recent field of topological condensed matter, following hints that topology can play a role in nonlinear fine-tuned mechanical systems [1], Kane and Lubensky [2] uncovered a connection between topological insulators [3–6] and linearized ball-and-spring models. Given the importance in the field of metamaterials [7–21] and magnetics [22,23], they realized if constraints define the system, zero modes (ZMs) can be topologically protected by a TKNN-like topological invariant [24].

It was quickly realized that Kane and Lubensky's ZMs in the case of a chain model they construct can survive back into the nonlinear regime and become bulk solitons [25]. But a formally identical origami system was identified that does not exhibit these solitons [26]. More nonlinear ZMs were found in mechanical systems in numerical simulations [27,28]. In a one-dimensional chain, a domain wall separating two distinct polarizations can be identified by constructing a sequence of consecutive maps on the space of ZMs of a single unit cell [29]. However, that does not quite guarantee that this domain wall can move continuously along the chain like a soliton. Thus, the existence of a soliton relies on the exact parameters of a model [30]. To the best of our knowledge, however, it remains unclear if solitons observed in generic mechanical systems are always topologically protected or not, and if so, what is the topology to classify them?

In this Letter, we develop an exact theory to study the topological protection of the kinematics of periodic mechanisms satisfying holonomic constraints such as those that arise in, e.g., linkages and origami. Using the concept of differential geometry, our theory predicts the existence of a \mathbb{Z} -type topological index μ or ν . To illuminate its applications, we further use this topological index to generate another topological index we call I that reveals whether or not a topologically protected ZM can propagate through the system. Applying this to the Kane-Lubensky (KL) chain, we realize the topology to classify the (two) distinct phases of the KL chain, namely the "flipper" and the "spinner," and further show that the existence of the spinner soliton is topologically protected and robust to disorders (unlike the flipper). In distinction, the origami chain does not support any soliton despite the superficial similarity of its linear ZMs to those of the KL chain.

We start by characterizing the type of mechanical system we are interested in. We assume that the state of the system can be described by generalized degrees of freedom, $\boldsymbol{\theta} = (\theta_1, \theta_2, ..., \theta_n)$, and that the system is characterized by a set of (spring) extensions $\mathbf{e}(\boldsymbol{\theta}) = [e_1(\boldsymbol{\theta}), ..., e_m(\boldsymbol{\theta})]$. While the elastic energy of such a system can be written as $E(\boldsymbol{\theta}) = \sum_i k_i e_i(\boldsymbol{\theta})^2$ for a set of moduli $k_i > 0$, here we will be interested only in the ground state configurations specified by $\bar{\boldsymbol{\theta}}$ such that $\mathbf{e}(\bar{\boldsymbol{\theta}}) = \mathbf{0}$. If we work with a mechanical linkage or a spring network as in Ref. [2], we can think of $\boldsymbol{\theta}$ representing the positions of the vertices of our network and $e_i(\boldsymbol{\theta})$ the extension of the springs (from their equilibrium lengths). In this language, the Jacobian $\partial e_i(\boldsymbol{\theta})/\partial \theta_i$ is termed the rigidity matrix.

Before presenting our prescription of defining topological indices, it is useful to review two examples that pose

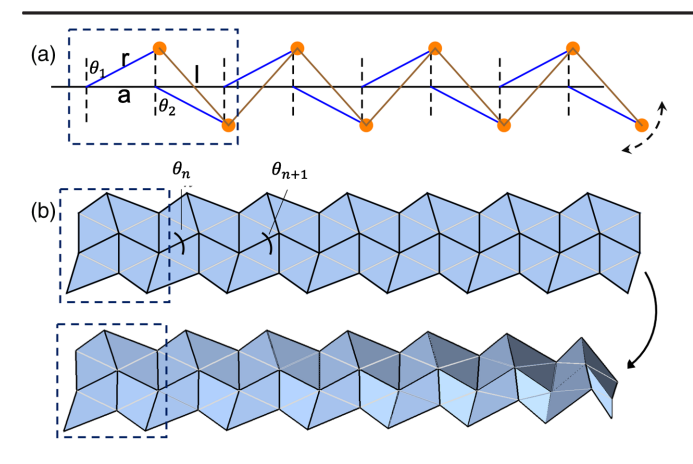


FIG. 1. (a) The KL chain has an edge mode on either the left or right edge. (b) The origami chain has an edge mode on either the left or right edge.

some apparent paradoxes in defining the topological invariant of the linear ZMs. First, for the KL chain, it is often easier to express the generalized coordinates in terms of the rotation angle of a series of rotors so that θ_i is the angle between the *i*th rotor and the vertical axis as shown in Fig. 1(a). The extension of the *i*th spring that connects the *i*th rotor with the (i + 1)th rotor and then takes the form $e_i(\theta) = f(\theta_i, \theta_{i+1})$, where

$$f(\theta_{i}, \theta_{i+1}) = [(a + r\sin\theta_{i+1} - r\sin\theta_{i})^{2} + (r\cos\theta_{i+1} + r\cos\theta_{i})^{2}]^{1/2} - L, \quad (1)$$

where a, r, and L are the distance between two consecutive pivot points, the radius of the rotors, and the equilibrium length of the springs, respectively. For an open chain of n springs (and n+1 rotors), if we choose $\theta_{n+1}=\theta_1$, then we have exactly as many constraints as the degrees of freedom, making the system isostatic.

In the second example of the origami chain [26], we instead use θ_i to denote the supplement of the dihedral angle of one of the folds of each vertex, also called the fold angle [Fig. 1(b)]. In this case,

$$f(\theta_i, \theta_{i+1}) = A\sin^2(\theta_i/2) - B\sin^2(\theta_{i+1}/2) + \epsilon, \quad (2)$$

where 0 < A < 1, 0 < B < 1, and ϵ are defined in Ref. [31]. Although it is straightforward to generalize the above equations to any periodic structure, for simplicity we specialize to the examples mentioned above focusing on Eqs. (1) and (2) for the remainder of this Letter.

In both the KL chain and the origami chain, if we assume a uniform solution of $\mathbf{e}(\bar{\boldsymbol{\theta}}) = \mathbf{0}$, following Ref. [2], the polarization is defined as the integer

$$Q = \frac{1}{2\pi i} \int_{\pi}^{\pi} dq \frac{\partial}{\partial q} \ln \left[\partial_1 f(\bar{\theta}, \bar{\theta}) + \partial_2 f(\bar{\theta}, \bar{\theta}) e^{iq} \right], \quad (3)$$

where ∂_a implies the derivative with respect to the ath variable in the argument of f. When $|\partial_2 f(\bar{\theta}, \bar{\theta})| > |\partial_1 f(\bar{\theta}, \bar{\theta})|$, Q = 0 and when $|\partial_2 f(\bar{\theta}, \bar{\theta})| < |\partial_1 f(\bar{\theta}, \bar{\theta})|$, Q = 1. These two values of Q define two distinct topological phases. For finite systems, the bulk is rigid for both Q = 0 and 1; however, the feature that distinguishes these two phases is the location of the linear ZM.

The behavior above is exhibited by the linear ZMs in both the KL chain and the origami chain, as it should. But in the KL chain (and not the origami chain), certain nonlinear deformations can propagate across the system, resulting in the edge mode appearing on the other side. In that sense, the polarization defined by Eq. (3), though an integer, is not necessarily topologically robust.

A topological index for isostatic systems.—To understand why the two models discussed above behave so differently in the presence of nonlinearity, we introduce a prescription to define topological indices in terms of the Poincaré-Hopf index [32] that accommodates nonlinear constraints as well. The definition of the index involves a generic nonlinear map $\mathbf{e}(\boldsymbol{\theta})$ [Eqs. (1) and Eq. (2) are two examples we are focused on in this work] that can be thought of as the vector field on the space of generalized coordinates as shown in Fig. 2(a). In the isostatic case (m=n), for a solution $\bar{\boldsymbol{\theta}}$ satisfying $\mathbf{e}(\bar{\boldsymbol{\theta}})=\mathbf{0}$, we can define an index $\mu(\bar{\boldsymbol{\theta}})$ by computing the winding number of the map $\mathbf{e}(\boldsymbol{\theta})$ on the (n-1)-dimensional sphere enclosing $\bar{\boldsymbol{\theta}}$, $S_{\bar{\boldsymbol{\theta}}}$ by integrating the differential form

$$\mu(\bar{\boldsymbol{\theta}}) = \frac{1}{(n-1)! A_{n-1}} \oint_{S_{\bar{\boldsymbol{\theta}}}} \frac{e_{i_1} de_{i_2} \wedge \dots \wedge de_{i_n} e^{i_1, i_2, \dots, i_n}}{(e_1^2 + e_2^2 + \dots + e_n^2)^{n/2}}, \quad (4)$$

where A_{n-1} is the surface area of a unit (n-1)-dimensional sphere. When, for example, n=2, it yields the so-called

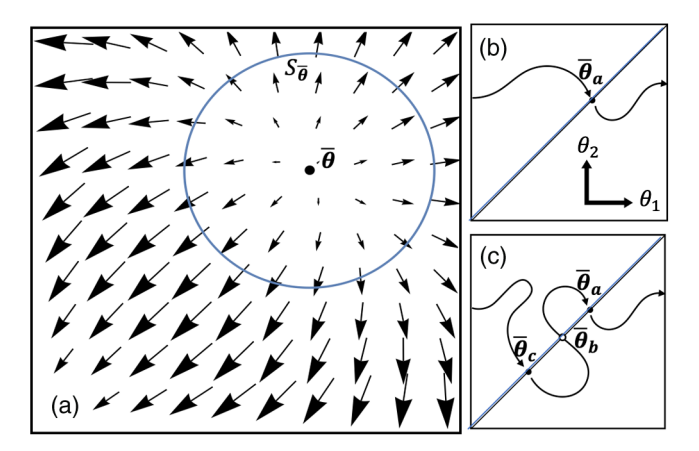


FIG. 2. (a) The vector field $\mathbf{e}(\bar{\boldsymbol{\theta}})$ is indicated by arrows. The winding number $\mu(\bar{\boldsymbol{\theta}})$ is a topological index that measures how many times the vector field rotates along $S_{\bar{\boldsymbol{\theta}}}$. (b) The total intersection number I is a homotopy invariant of a ZM and counts the minimal number of periodic configurations along that ZM. (c) A ZM with a deformed trajectory has the same total intersection number as (b).

first Chern number, which frequently appears in classifying the topology in electronic band structures. $\mu(\bar{\theta})$ is well defined for any isolated solution $\bar{\theta}$ even when the Jacobian is not full rank. It is also known as the degree of a map [33], which implies $\mu(\bar{\theta})$ predicts the minimum number of nonlinear ZMs that would pass through the configuration $\bar{\theta}$ after releasing one constraint.

When the Jacobian is full rank, $\mu(\bar{\theta}) = \text{sgn}[\det(\partial e_i(\bar{\theta})/\partial \theta_j)]$ [34]. Under this condition, the configuration $\bar{\theta}$ is structurally stable, meaning that $\mu(\bar{\theta})$ is invariant under small, continuous deformations of the constraint functions $\mathbf{e}(\theta)$. The idea of topological protection in a linear theory can now be cast as the following: without any symmetry, the phonon spectrum is characterized by a \mathbb{Z}_2 invariant protected by a bulk gap that closes when the Jacobian is not full rank.

A deeper physical meaning of $\mu(\bar{\theta})$ relies on the form of constraints. For example, in the KL and origami chain with periodic boundary conditions, for a uniform solution $\bar{\theta}$, $\mu_{PBC}(\bar{\theta})$ can be simplified to $\mu_{PBC}(\bar{\theta}) = \text{sgn}\{[\partial_1 f(\bar{\theta},\bar{\theta})]^n - [-\partial_2 f(\bar{\theta},\bar{\theta})]^n\}$, which depends only on the magnitude of $\partial_1 f(\bar{\theta},\bar{\theta})$ and $\partial_2 f(\bar{\theta},\bar{\theta})$. Consequently, $\mu_{PBC}(\bar{\theta}) = 1$ when $|\partial_1 f(\bar{\theta},\bar{\theta})| > |\partial_2 f(\bar{\theta},\bar{\theta})|$ and $\mu_{PBC}(\bar{\theta}) = -1$ when $|\partial_1 f(\bar{\theta},\bar{\theta})| < |\partial_2 f(\bar{\theta},\bar{\theta})|$. Therefore, $\mu_{PBC}(\bar{\theta}) = 2Q - 1$, where Q is the topological polarization discovered by Kane and Lubensky [2].

A topological index for nonisostatic systems.—So far, the topological index μ discussed above applies only to an isolated zero-energy configuration $\bar{\theta}$ in an isostatic system. To capture the topology of a nonlinear ZM in a nonisostatic system, we now extend our consideration to derive another similar topological index ν . To do so, we look at this topological index from another perspective by first defining a tangent d-form

$$T^{i_1\cdots i_d} = \epsilon^{i_1\cdots i_d j_1\cdots j_{n-d}} \partial_{i_1} e_1 \cdots \partial_{i_{n-d}} e_{n-d}, \tag{5}$$

where d denotes the dimension of the nonlinear ZM. Because $T^{i_1\cdots i_d}(\boldsymbol{\theta}_{i_1}\cdots\boldsymbol{\theta}_{i_d})=0$ for any vector $\boldsymbol{\theta}_{i_i}$ normal to the space of ZMs, we can think of $T^{i_1 \cdots i_d}$ as defining the tangent space of nonlinear ZMs. For an open KL chain, the number of constraints is one less than the number of the degrees of freedom, and so d = 1. Then T is a vector field that is everywhere tangent to a nonlinear ZM. In this case, the nonlinear ZM can be found as the solution to the first-order differential equation $\partial_s \theta(s) = T[\theta(s)]$. So long as $T(\theta)$ is a smooth nonvanishing function of θ , the integral curves of $T(\theta)$ will be smooth as well. For any surface not parallel to the tangent $T(\theta)$, we can define an intersection number at the point $\bar{\theta}$ where the ZM intersects with the surface as $\nu(\bar{\theta}) = \text{sgn}[T(\bar{\theta}) \cdot \hat{N}(\bar{\theta})]$, where $\hat{N}(\bar{\theta})$ is the unit normal to the surface at $\bar{\theta}$. Alternatively, we can define a vector $\mathbf{g}(\boldsymbol{\theta}) = (e_1, e_2, ..., e_{n-1}, h)$, where h is the function describing the surface. Then $\nu(\bar{\pmb{\theta}})$ can be computed as

$$\nu(\bar{\boldsymbol{\theta}}) = \frac{1}{(n-1)! A_{n-1}} \oint_{S_{\bar{u}}} \frac{g_{j_1} dg_{j_2} \wedge \dots \wedge dg_{j_n} \epsilon^{j_1 j_2 \dots j_n}}{(g_1^2 + g_2^2 + \dots + g_n^2)^{n/2}}, \quad (6)$$

similar to the way μ was defined earlier in Eq. (4). This results in $\nu(\bar{\theta}) = \mathrm{sgn}[\det \nabla g(\bar{\theta})]$ when the Jacobian of g, denoted $\nabla g(\bar{\theta})$, is full rank. The function h can also be thought as an auxiliary constraint used to obtain information of a nonlinear ZM. For example, in the KL and origami chain, when $h = e_n = f(\theta_n, \theta_1)$ as defined previously, $\nu(\bar{\theta})$ would be $\mu_{PBC}(\bar{\theta})$.

Topological distinctions between the KL chain and origami chain.—Based on the earlier discussion of μ , there always exists at least one nonlinear ZM passing through a uniform solution in both the open KL and open origami chain because $\mu_{PBC} = \pm 1$ for each uniform solution in both cases. However, to understand whether this nonlinear ZM can propagate from one site to another, we need to specialize to a local topological index $\nu_{loc}(\bar{\theta})$ in a single cell (which contains two sites with one constraint) with a twodimensional space specified by (θ_1, θ_2) and consider h specified by $\theta_2 - \theta_1 = 0$. In this example, every time the nonlinear ZM for a single cell (SCZM) crosses this plane at $\bar{\boldsymbol{\theta}}$, we can associate an index $\nu_{\mathrm{loc}}(\bar{\boldsymbol{\theta}})$ with the intersection point as defined above [see Fig. 2(b)]. With this in mind, for continuous deformations of the trajectory of the SCZM [see Fig. 2(c)], new uniform configurations can be created or annihilated in pairs of opposite indices, but the total intersection number $I = \sum_{i} \nu_{loc}(\boldsymbol{\theta}_{i})$ of the SCZM remains invariant.

The idea of topological protection, defined as it is in terms of an inherently linear concept of the phonon spectrum as highlighted before, can be carried over in a robust way to nonlinear mechanical systems as follows: the space of ZMs for one set of constraints can be continuously deformed into the space of ZMs of another set of constraints as long as no ZM intersects with others or itself during deformations. Then it will become clearer why the KL chain and the origami chain behave so differently despite their superficial similarity after computing the intersection number of a single cell.

First, Figs. 3(a) and 3(b) show the solutions to Eq. (1) for a single cell of the KL chain (consisting of a pair of rotors). Uniform solutions, namely $\theta_1 = \theta_2$ (there are four), correspond to the points where the nonlinear SCZMs cross the plane $\theta_1 - \theta_2 = 0$. We note that, in the nonlinear model, the trajectory of a nonlinear SCZM passes through either two or all four of these (uniform) solutions depending on the values of L, r, and a. The total intersection number I of a nonlinear SCZM satisfies the following condition: when a < L < 2r - a, there are two distinct SCZMs with I = +2 [blue in Fig. 3(a)] and I = -2 [red in Fig. 3(a)].

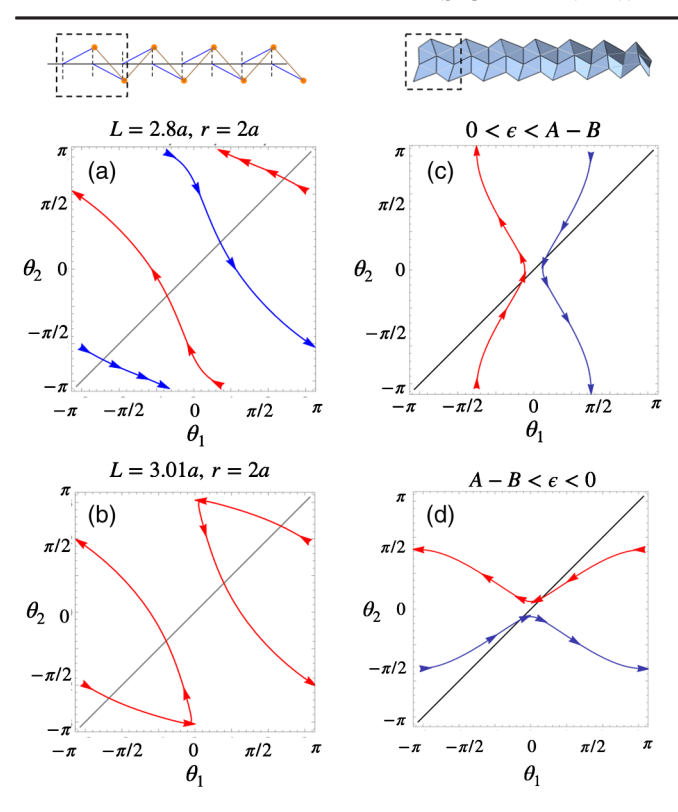


FIG. 3. (a),(b) are the spaces of ZMs of a single cell for the KL chain. (c),(d) are the spaces of ZMs of a single cell for the origami chain. The color is only a label (blue for I > 0 and red for $I \le 0$) and does not have a quantitative meaning.

Thus, each SCZM passes two distinct uniform solutions at least twice and these two uniform solutions are necessarily connected via the trajectory of the SCZM. This case is known as the "spinner" phase of the KL chain, characterized by spinner solitons whose existence is topologically protected. When 2r - a < L < 2r + a, on the other hand, we have only one SCZM with a total intersection number I = 0 [this SCZM passes through all four solutions as in Fig. 3(b)]. This is dubbed the "flipper" phase. In this phase, the trajectory of the SCZM can be continuously deformed by tuning, e.g., L, such that all four solutions get annihilated in pairs of opposite intersection numbers exactly at L = 2r + a, and no solution exists beyond that.

Next, we consider the origami chain. A single cell in this model is described by Eq. (2). The uniform solutions are given by the zeros of $f(\theta,\theta)=(A-B)\sin^2(\theta/2)+\epsilon$, which exist only when $(B-A)/\epsilon>1$. As shown in Figs. 3(c) and 3(d), there are two distinct regimes: (i) $0<\epsilon< A-B$ and (ii) $A-B<\epsilon<0$, both of which have two uniform solutions with opposite sign of ν_{loc} and the two SCZMs correspond to the total intersection number of I=+1 [blue in Fig. 3(c) or 3(d)] or I=-1 [red in Fig. 3(c) or 3(d)]. As seen in Figs. 3(c) and 3(d), each SCZM crosses the line defined by $\theta_1=\theta_2$ at least once. If the system is distorted, it is possible to cross this line multiple times, but the total intersection number remains

unchanged. We conclude that the existence of uniform solutions is, indeed, topologically protected. To eliminate them, it is necessary to distort the system through a topological phase transition by joining the trajectories of the two SCZMs. Ultimately, this requires tuning the system through one of the two situations: $\epsilon = 0$ or $A - B + \epsilon = 0$.

It is clear that when a SCZM has a total intersection number $|I| \ge 2$, it must have at least two uniform solutions joined by a smooth trajectory. However, this does not immediately extend to a larger chain of n (n > 2) unless the following (sufficient) condition P is met: for a given SCZM, either the map from θ_i to $\theta_{i+1} \ \forall \ i$ or the reverse map is injective.

Lets take the spinner for an example and denote a ZM for the n-site chain, which contains n rotors and n-1 springs, by C_n . In this notation, the black curve on the bottom plane in Fig. 4(a) is C_2 and the red curve is C_3 . Because in this case we have |I|=2, the projection of C_3 onto a constant θ_3 plane always yields C_2 (it, in fact, extends to $|I| \geq 2$). This statement can be understood in the following way: We are looking for a solution for $f(\theta_2,\theta_3)=0$ provided $f(\theta_1,\theta_2)=0$. A sufficient condition for this is that the solution of $f(\theta_2,\theta_3)=0$ on the $\theta_2-\theta_3$ plane wraps

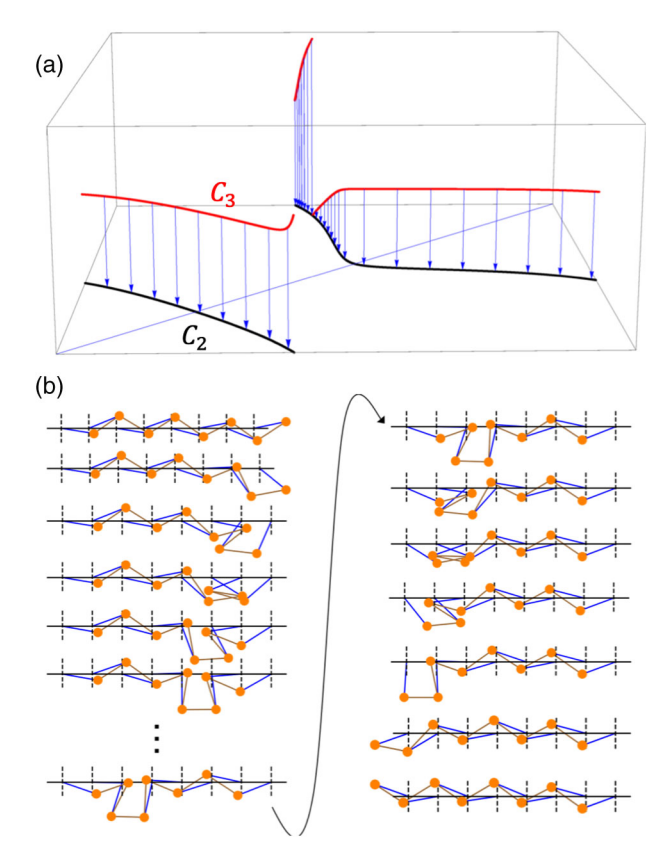


FIG. 4. (a) The ZM for the n=2, 3 KL chain (the spinner case). The black curve C_2 on the bottom plane is a single loop on a two-dimensional torus, and the red curve C_3 is a single loop on a three-dimensional torus. (b) A soliton on the disordered KL chain.

around θ_2 at least once (this holds when $|I| \ge 2$), guaranteeing a θ_3 for a given θ_2 that also satisfies $f(\theta_1, \theta_2) = 0$. If the above condition is met, there must exist at least one θ_3 for a given (θ_1, θ_2) that satisfies both the constraints. Thus, for each point on the black curve C_2 , we can always find at least one point on the red curve C_3 projected onto it.

We can now prove that the two uniform solutions are connected by C_3 , which we have shown to hold for C_2 previously. This we prove by contradiction. If we assume that there are two disconnected parts of C_3 while C_2 is connected, there must exist two points that have the same θ_1 and θ_2 but distinct θ_3 . However, this contradicts the fact that the map from θ_3 to θ_2 is injective, and thus C_3 must be connected. The argument can easily be generalized to C_n for n > 3. Thus, we conclude that there must exist at least two uniform solutions joined by a ZM in a *n*-site chain. This ZM is a soliton (for the nonlinear model) that is topologically protected and robust to disorders as long as each SCZM corresponds to a total intersection number $|I| \ge 2$ and satisfies the condition P mentioned above. We emphasize, a soliton of this kind exists even in a disordered $(a < L_i < 2r - a, L_i$ chosen randomly) KL chain that has the total intersection number $I = \pm 2$ in each cell as shown in Fig. 4(b).

We conclude by emphasizing that new topological indices can be generated in similar manners following our prescription to classify nonlinear ZMs. For instance, a n-1-dimensional sphere around an isolated zero-energy configuration (solution) is chosen in this work as the base manifold to construct a bundle with \mathbb{Z} -type topological invariant. For higher-dimensional manifolds of such solutions, different choices of the base manifold can lead to different types of topological invariants [35]. Exploring the physical significance of those topological indices constitutes a new direction of searching for novel topologically protected nonlinear ZMs in the future.

B. G. C. and C. D. S. were partially supported by EFRI Grant No. 1240441. B. G. C. was partially supported by NSF Award No. PHY-1554887. C. D. S. was partially supported by DMR Grant No. 1822638. K. R. thanks the Swedish Research Council for sponsorship in part.

- [1] M. J. Lawler, Emergent gauge dynamics of highly frustrated magnets, New J. Phys. **15**, 043043 (2013).
- [2] C. L. Kane and T. C. Lubensky, Topological boundary modes in isostatic lattices, Nat. Phys. **10**, 39 (2014).
- [3] L. Fu and C. L. Kane, Topological insulators with inversion symmetry, Phys. Rev. B **76**, 045302 (2007).
- [4] R. Roy, Z_2 classification of quantum spin hall systems: An approach using time-reversal invariance, Phys. Rev. B **79**, 195321 (2009).
- [5] C. L. Kane and E. J. Mele, Z₂ Topological Order and the Quantum Spin Hall Effect, Phys. Rev. Lett. 95, 146802 (2005).

- [6] M.Z. Hasan and C.L. Kane, Colloquium: Topological insulators, Rev. Mod. Phys. **82**, 3045 (2010).
- [7] T. C. Lubensky, C. L. Kane, X. Mao, A. Souslov, and K. Sun, Phonons and elasticity in critically coordinated lattices, Rep. Prog. Phys. 78, 073901 (2015).
- [8] J. Paulose, B. Gin-ge Chen, and V. Vitelli, Topological modes bound to dislocations in mechanical metamaterials, Nat. Phys. 11, 153 (2015).
- [9] J. Paulose, A. S. Meeussen, and V. Vitelli, Selective buckling via states of self-stress in topological metamaterials, Proc. Natl. Acad. Sci. U.S.A. 112, 7639 (2015).
- [10] Z. Yang, F. Gao, X. Shi, X. Lin, Z. Gao, Y. Chong, and B. Zhang, Topological Acoustics, Phys. Rev. Lett. 114, 114301 (2015).
- [11] L. M. Nash, D. Kleckner, A. Read, V. Vitelli, A. M. Turner, and W. T. M. Irvine, Topological mechanics of gyroscopic metamaterials, Proc. Natl. Acad. Sci. U.S.A. 112, 14495 (2015).
- [12] P. Wang, L. Lu, and K. Bertoldi, Topological Phononic Crystals with One-Way Elastic Edge Waves, Phys. Rev. Lett. 115, 104302 (2015).
- [13] Y.-T. Wang, P.-G. Luan, and S. Zhang, Coriolis force induced topological order for classical mechanical vibrations, New J. Phys. 17, 073031 (2015).
- [14] R. Süsstrunk and S. D. Huber, Observation of phononic helical edge states in a mechanical topological insulator, Science 349, 47 (2015).
- [15] P. Wang, L. Lu, and K. Bertoldi, Topological Phononic Crystals with One-Way Elastic Edge Waves, Phys. Rev. Lett. 115, 104302 (2015).
- [16] H. C. Po, Y. Bahri, and A. Vishwanath, Phonon analog of topological nodal semimetals, Phys. Rev. B 93, 205158 (2016).
- [17] D. Zeb Rocklin, B. Gin-ge Chen, M. Falk, V. Vitelli, and T. C. Lubensky, Mechanical Weyl Modes in Topological Maxwell Lattices, Phys. Rev. Lett. 116, 135503 (2016).
- [18] O. Stenull, C. L. Kane, and T. C. Lubensky, Topological Phonons and Weyl Lines in Three Dimensions, Phys. Rev. Lett. **117**, 068001 (2016).
- [19] L. Zhang and X. Mao, Fracturing of topological maxwell lattices, New J. Phys. 20, 063034 (2018).
- [20] A. Saremi and Z. Rocklin, Controlling the deformation of metamaterials: Corner modes via topology, Phys. Rev. B 98, 180102 (2018).
- [21] D. Zhou, L. Zhang, and X. Mao, Topological Boundary Floppy Modes in Quasicrystals, Phys. Rev. X 9, 021054 (2019).
- [22] K. Roychowdhury, D. Zeb Rocklin, and M. J. Lawler, Topology and Geometry of Spin Origami, Phys. Rev. Lett. 121, 177201 (2018).
- [23] K. Roychowdhury and M. J. Lawler, Classification of magnetic frustration and metamaterials from topology, Phys. Rev. B 98, 094432 (2018).
- [24] D. J. Thouless, M. Kohmoto, M. P. Nightingale, and M. den Nijs, Quantized Hall Conductance in a Two-Dimensional Periodic Potential, Phys. Rev. Lett. **49**, 405 (1982).
- [25] B. Gin-ge Chen, N. Upadhyaya, and V. Vitelli, Non-linear conduction via solitons in a topological mechanical insulator, Proc. Natl. Acad. Sci. U.S.A. 111, 13004 (2014).

- [26] B. Gin-ge Chen, B. Liu, A. A. Evans, J. Paulose, I. Cohen, V. Vitelli, and C. D. Santangelo, Topological Mechanics of Origami and Kirigami, Phys. Rev. Lett. 116, 135501 (2016).
- [27] J. Paulose, A. S. Meeussen, and V. Vitelli, Selective buckling via states of self-stress in topological metamaterials, Proc. Natl. Acad. Sci. U.S.A. 112, 7639 (2015).
- [28] D. Zhou, L. Zhang, and X. Mao, Topological Edge Floppy Modes in Disordered Fiber Networks, Phys. Rev. Lett. 120, 068003 (2018).
- [29] Y. Zhou, B. Gin-ge Chen, N. Upadhyaya, and V. Vitelli, Kink-antikink asymmetry and impurity interactions in topological mechanical chains, Phys. Rev. E 95, 022202 (2017).

- [30] K. Sato and R. Tanaka, Solitons in one-dimensional mechanical linkage, Phys. Rev. E 98, 013001 (2018).
- [31] See Supplemental Material at http://link.aps.org/ supplemental/10.1103/PhysRevLett.127.076802 for the details of the origami chain.
- [32] J.-P. Brasselet, J. Seade, and T. Suwa, *Vector Fields on Singular Varieties* (Springer-Verlag, Berlin Heidelberg, 2009).
- [33] P. Olum, Mappings of manifolds and the notion of degree, Ann. Math. **58**, 458 (1953).
- [34] I. Fonseca, N. Fusco, and P. Marcellini, Topological degree, jacobian determinants and relaxation, Bollettino dell'Unione Mat. Italiana **8-B**, 187 (2005).
- [35] M. F. Atiyah, *K-theory (Advanced Book Classics)* (Addison-Wesley, Reading, MA, 1989).

Supplemental Material: Topology in non-linear mechanical systems

Po-Wei Lo,¹ Christian D Santangelo,² Bryan Gin-ge Chen,³
Chao-Ming Jian,¹ Krishanu Roychowdhury,⁴ and Michael J Lawler^{1,5}

¹Laboratory of Atomic and Solid State Physics, Cornell University, Ithaca, NY, 14853

²Department of Physics, Syracuse University, Syracuse, NY, 13244

³Lorentz Institute for Theoretical Physics, Leiden University, Leiden 2333 CA, Netherlands

⁴Department of Physics, Stockholm University, SE-106 91 Stockholm, Sweden

⁵Department of Physics, Applied Physics and Astronomy,

Binghamton University, Binghamton, New York 13902

(Dated: June 10, 2021)

PACS numbers:

Appendix A: The origami chain

The origami chain is a periodic origami fold pattern of degree-4 vertices constructed from quadrilaterals as shown in Fig. 1. Each vertex, because it has a one-dimensional configuration space, can be parametrized by the fold angle of a single vertex so any finite number of vertices will have one degree of freedom. There are two degree-4 vertices in each unit cell with interior angles $\{\alpha_i, \beta_i, \phi_i, \psi_i\}$ for the i^{th} vertex. When the interior angles around each internal vertex add up to 2π , the fold pattern can be realized as a flat structure; here, we will extend the calculation of Ref.1 to the more general case of arbitrary interior angles.

The law of cosines applied to each vertex gives a constraint on the dihedral angles θ as,

$$\cos(\alpha_1)\cos(\psi_1) + \sin(\alpha_1)\sin(\psi_1)\cos\theta_1 = \cos(\beta_1)\cos(\phi_1) + \sin(\beta_1)\sin(\phi_1)\cos\theta_2$$
$$\cos(\alpha_2)\cos(\psi_2) + \sin(\alpha_2)\sin(\psi_2)\cos\theta_2 = \cos(\beta_2)\cos(\phi_2) + \sin(\beta_2)\sin(\phi_2)\cos\theta_3$$

After some manipulation, we obtain

$$A\sin^2\left(\frac{\delta\theta_1}{2}\right) - B\sin^2\left(\frac{\delta\theta_2}{2}\right) + \epsilon = 0,\tag{A1}$$

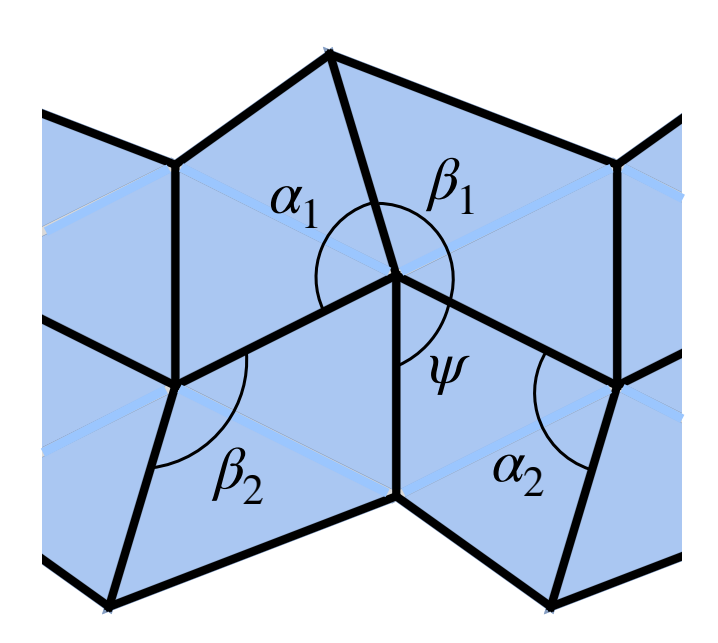


FIG. 1: The origami topological chain.

where $\delta\theta_i = \pi - \theta_i$ and

 $A = \sin \alpha_{1} \sin \alpha_{2} \sin \psi_{1} \sin \psi_{2},$ $B = \sin \beta_{1} \sin \beta_{2} \sin \phi_{1} \sin \phi_{2},$ $2\epsilon = \sin(\alpha_{2}) \sin(\psi_{2}) \left[\cos(\alpha_{1} + \psi_{1}) - \cos(\beta_{1}) \cos(\phi_{1})\right] + \sin(\beta_{1}) \sin(\phi_{1}) \left[\cos(\alpha_{2}) \cos(\phi_{2}) - \cos(\beta_{2} + \phi_{2})\right].$

When the Gaussian curvature of both vertices is zero, $\epsilon = 0$.

¹ T. C. Lubensky, C. L. Kane, Xiaoming Mao, A. Souslov, and Kai Sun. Phonons and elasticity in critically coordinated lattices. *Reports on Progress in Physics*, 78(7):1 – 30, July 2015.